Published in final edited form as:
J Control Release. 2012 April 10; 159(1): 52–59. doi:10.1016/j.jconrel.2012.01.003.

Dissolving polymeric microneedle arrays for electrically assisted transdermal drug delivery

Martin J. Garland, **Ester Caffarel–Salvador**, **Katarzyna Migalska**, **A. David Woolfson**, and **Ryan F. Donnelly***
School of Pharmacy, Queen's University Belfast, Medical Biology Centre, 97 Lisburn Road, Belfast BT9 7BL, UK

Abstract

It has recently been proposed that the combination of skin barrier impairment using microneedles (MNs) coupled with iontophoresis (ITP) may broaden the range of drugs suitable for transdermal delivery, as well as enabling the rate of delivery to be achieved with precise electronic control. However, no reports exist on the combination of ITP with *in situ* drug loaded polymeric MN delivery systems. Furthermore, although a number of studies have highlighted the importance of MN design for transdermal drug delivery enhancement, to date, there has been no systematic investigation of the influence of MN geometry on the performance of polymeric MN arrays which are designed to remain in contact with the skin during the period of drug delivery. As such, for the first time, this study reports on the effect of MN heigth and MN density upon the transdermal delivery of small hydrophilic compounds (theophylline, methylene blue, and fluorescein sodium) across neonatal porcine skin *in vitro*, with the optimised MN array design evaluated for its potential in the electrically faciliatated delivery of peptide (bovine insulin) and protein (fluorescein isothiocyanate—labelled bovine serum albumin (FTIC-BSA)) macromolecules. The results of the *in vitro* drug release investigations revealed that the extent of transdermal delivery was dependent upon the design of the MN array employed, whereby an increase in MN height and an increase in MN density led to an increase in the extent of transdermal drug delivery achieved 6 h after MN application. Overall, the *in vitro* permeation studies revealed that the MN design containing 361 MNs/cm^2 of 600 μm height resulted in the greatest extent of transdermal drug delivery. As such, this design was evaluated for its potential in the MN mediated iontophoretic transdermal delivery. Whilst the combination of MN and ITP did not further enhance the extent of small molecular weight solute delivery, the extent of peptide/protein release was significantly enhanced when ITP was used in combination of the soluble PMVE/MA MN arrays. For example, the cumulative amount of insulin permeated across neonatal porcine skin at 6 h was found to be approximately 150 μg (3.25%), 227 μg (4.85%) and 462 μg (9.87%) for ITP, MN, and MN/ITP delivery strategies, respectively. Similarly, the cumulative amount of FTIC-BSA delivered across neonatal porcine skin after a 6 h period was found to be approximately 110 μg (4.53%) for MN alone and 326 μg (13.40%) for MN in combination with anodal ITP (p<0.001). As such, drug loaded soluble PMVE/MA MN arrays show promise for the electrically controlled transdermal delivery of biomacromolecules in a simple, one-step approach.

*Corresponding author. Tel.: +44 28 90 972 251; fax: +44 28 90 247 794. r.donnelly@qub.ac.uk (R.F. Donnelly) .

Europe PMC Funders Author Manuscripts

Keywords

Microneedles; Iontophoresis; Transdermal drug delivery

1. Introduction

The rapid growth of the biotechnology industry has seen an increase in the interest for use of peptide/protein based molecules as therapeutic agents [1]. In order for this new generation of therapeutic agents to gain prominence as mainstream treatments of choice, a parallel development of efficient delivery systems will be required by the pharmaceutical industry [2]. Traditionally, peptide and protein drugs have had to be administered parenterally, due to their propensity to undergo acid degradation within the gastrointestinal tract [3]. However, recent advances have seen the development of facilitated technologies that may make transdermal peptide/protein delivery a feasible option. The transdermal route offers a range of advantages for delivery of peptide/protein therapeutics. As proteins have short plasma half-lives, the possibility of continuous delivery offered by the transdermal route is a major benefit, as is the low proteolytic activity in comparison to other routes [1,2]. Furthermore, avoidance of first pass hepatic metabolism eliminates another obstacle to successful systemic peptide/protein delivery. The major challenge associated with delivery of molecules across the skin is overcoming the *stratum corneum* barrier. Thus, a number of enhancement methods have been proposed and investigated to improve bioavailability of peptides/proteins administered across the skin.

The development of microneedle (MN) arrays is likely to play a major role in the progression of the transdermal route as a viable option for the non-invasive systemic delivery of therapeutic peptide/protein agents. MNs are devices composed of micron-size needles which have the ability to physically disrupt the SC and create micro-conduits for drugs to pass through deeper layers of the skin to the microcapillary bed for systemic absorption [2]. MN technology has been demonstrated to be painless [4] and associated with only very minor local adverse skin reactions [5,6]. As such MN technology appears to be an attractive minimally invasive and patient-friendly drug delivery option for macromolecular therapeutics. MNs have been fabricated in a wide range of designs from various materials, including silicon [7], glass [8], metal [9] and polymers [10–12].

Recently, it has been suggested that, due to the fact that MN application to the skin will result in the creation of aqueous pathways of low electrical resistance [13], the combination of MN technologies and iontophoresis (the application of a small electric current, typically≥0.5 mA/cm^2, to drive ionic and polar molecules across the skin) may lead to a synergistic enhancement in transdermal delivery with the added benefit of precise electronic control [14,15]. Indeed it has been shown that the combination of MN and ITP can lead to an increased rate of transdermal delivery for a range of drug molecules, both *in vitro* and *in vivo* [13,15–17]. However, to date the combination of ITP and MNs has focused on the use of either non-drug loaded solid MNs that are used to merely puncture the skin prior to the application of an electrically conducting drug formulation, or the use of an electric stimulus to facilitate drug movement through the cental bore of hollow MNs. In these cases, the pores

created within the skin could potentially close or, in the case of the hollow MNs the central bore may become blocked by compressed dermal tissue during MN insertion, thus negating the length of benefit that may be obtained through the use of ITP to stimulate drug movement. The use of drug loaded dissolving polymer MN systems may overcome some of the above mentioned issues, and thus allow for the *in situ* combination of MN and ITP in a one-step approach for enhanced transdermal delivery of a wide range of drug molecules.

Whilst a number of studies have highlighted the importance of MN design for transdermal drug delivery enhancement, to date, there has been no systematic investigation of the influence of MN geometry on the performance of polymeric MN arrays which are designed to remain in contact with the skin during the period of drug delivery. As such, for the first time, this study reports on the effect of MN height and MN density upon the transdermal delivery of small hydrophilic compounds (chosen for their ease of analysis, thus enabling a range of MN parameters to be evaluated in an efficient and rapid fashion) across neonatal porcine skin *in vitro*, with the optimised MN array design evaluated for its potential in the electrically faciliatated delivery of peptide (bovine insulin) and protein (fluorescein isothiocyanate—labelled bovine serum albumin (FTIC-BSA)) macromolecules.

2. Materials and methods

2.1. Chemicals

Gantrez® AN-139, a copolymer of methylvinylether and maleic anhydride (PMVE/MAH) was provided by ISP Co. 120 Ltd., Guildford, UK. Theophylline, methylene blue, fluorescein sodium, insulin from bovine pancreas and FTIC-BSA were obtained from Sigma Aldrich, Dorset, UK. All other chemicals used were of analytical reagent grade.

2.2. Fabrication of drug-loaded MNs prepared from aqueous blends of 20% w/w PMVE/MA

MNs prepared from aqueous blends of 20% w/w poly (methyl vinyl ether co maleic acid) (PMVE/MA) and loaded with model drugs were prepared using laser-engineered silicone micromould templates, as described previously [3,12]. Briefly, silicone elastomer (LSR9-9508-30, Polymer Systems Technology, Wycombe, UK) was poured into a custom-made aluminium mould and cured overnight at 40 °C. A laser-machine tool (BluLase® Micromachning System, Blueacre Technology, Dundalk, Ireland) with a laser (Coherent Avia, Coherent Inc., Pittsburgh, USA) emitting a beam having a wavelength of 355 nm and a pulse length of 30 ns (variable from 1 to 100 kHz) was then employed to produce MN moulds (11 × 11 array, 600 μm height, 300 μm width and 300 μm interspacing at MN base). A 30% w/w aqueous solution of PMVE/MA was prepared by adding the required mass of PMVE/MAH to ice-cold deionised water, followed by vigorous stirring and heating at 95.0 °C until a clear gel was obtained, due to hydrolysis of the anhydride form of the copolymer to the corresponding acid (PMVE/MA). Upon cooling, the blend was then readjusted to the final concentration of 30% w/w by addition of an appropriate amount of deionised water. To prepare drug-loaded MNs, the stock solution was diluted with the appropriate amount of water, in which the amount of model drugs necessary to obtain desired loadings per MN device (Table 1) was dissolved, to obtain MNs composed of 20% w/w PMVE/MA gel. In each case the model drugs were distributed throughout the entire of the MN array, i.e. drug

was contained both within the MNs and the MN base plate.An aliquot of 0.5 g of the obtained solution was then poured into the silicone micromould, centrifuged for 15.0 min at 3500 rpm and allowed to dry under ambient conditions for 24 h [12]. Control patches were prepared by pouring a 0.5 g aliquot of the drug loaded PMVE/MA gel into silicone micromoulds, containing no laser engineered MN holes, which were then allowed to dry under ambient conditions for 24 h [12]. In order to assess the effect of MN array design on the drug release characteristics of polymeric MNs containing small hydrophilic molecules, a range of MN geometries were prepared (Table 1).

2.3. Analysis of drug content after incorporation into PMVE/MA MN arrays

For evaluation of the drug content of drug loaded PMVE/MA MN arrays, MN arrays were dissolved in 0.1 M PBS pH 7.4 and analysed *via* UV/VIS spectroscopy for methylene blue and fluorescein sodium loaded MNs [18], *via* HPLC for theophylline [12] and insulin loaded MNs [3]. For the evaluation of the total FITC-BSA content in soluble PMVE/MA MN arrays, MN arrays were dissolved in 0.05% w/w sodium dodecyl sulphate (SDS) in PBS pH 7.4 and the obtained solutions were analysed using by spectrofluorimetry using an excitation wavelength of 490 nm and emission wavelength of 520 nm. Mean values were determined from a total of five replicates in each case.

2.4. In vitro permeation studies across neonatal porcine skin

In vitro drug delivery experiments were performed across dermatomed neonatal porcine skin (nominal thickness 350 μm), which was mounted on Franz diffusion cells (FDC-400 flat flange, 15 mm orifice diameter, mounted on an FDC diffusion drive console providing synchronous stirring at 600 rpm and thermostated at 37 ± 1 °C, Crown Glass Co. Inc., Sommerville, N.J., USA). Neonatal porcine skin was obtained from stillborn piglets and immediately (<24 h after birth) excised, and trimmed to a nominal thickness of 350 μm using an electric dermatome. Skin was then stored in aluminium foil at −20 °C until further use. Neonatal porcine skin samples were shaved carefully so as not to damage the skin and pre-equilibrated in phosphate buffered saline pH 7.4 (PBS) for 1 h before beginning the experiments. A circular specimen of the skin was secured to the donor compartment of the diffusion cell using cynoacrylate glue with the *stratum corneum* side facing the donor compartment. This was then placed on top of dental wax, to give the skin support, and MN arrays inserted into the centre of the skin section, using a spring activated applicator at a force of 11.0 N per array. A circular steel weight (diameter 11.0 mm, 3.5 g mass) was then placed on top of the MN array. Furthermore, a non-adhesive putty material (BluTac®, Bostik Ltd., Leicester, UK) was placed on top of the weight, and a piece of laboratory film (Parafilm®) placed over the Franz cell lid. With MN arrays in place, donor compartments were mounted onto the receptor compartments of the Franz cells.

For studies involving the application of an electric current, silver wire was used as an anode, with a silver-silver chloride electrode acting as the cathode The active electrode was placed directly on top of the MN array, whilst the inactive electrode was placed into the receiver medium *via* the side arm of the Franz cell (Fig. 1). A commercially available power supply (Phoresor II, Iomed, Lake City, FL, USA) was used to deliver a current of 0.5 mA for a 6 h period.

As a negative control, drug loaded patches (with the same drug loading but containing no MNs) were applied to skin using the spring-activated applicator at a force of 11.0 N/patch, and kept in place during the experiment by application of the non-adhesive putty.

At predetermined time intervals, a 300 μl sample was collected *via* the side arm of the Franz cell and the receiver compartment immediately replenished with an equivalent volume of release medium. For studies involving theophylline, methylene blue and fluorescein sodium phosphate buffered saline (PBS pH 7.4) was used as the release medium. For studies involving insulin, a release medium containing 0.1 M Tris buffer pH 10 was used to ensure stability of insulin during the course of Franz cell investigations [3]. For studies involving FTIC-BSA a release medium of 0.05% w/w SDS in PBS pH 7.4 (to ensure stability of FTIC-BSA) was used. The concentrations of methylene blue and fluorescein sodium within the receiver medium were determined by UV analysis, the concentration of theophylline and insulin within the receiver medium were determined by HPLC, and the concentration of FTIC-BSA within the receiver medium was determined by fluorescence spectroscopy.

2.5. Transcutaneous electrical resistance measurements

Full thickness neonatal porcine skin (1.0 mm) was mounted over a Franz diffusion cell with the receptor compartment containing phosphate buffered saline (pH 7.4). Ag/AgCl electrodes, connected to a multimeter, were placed on either side of the skin portion to measure the resistance in kΩ [13]. MN array were inserted into the skin using a custom designed spring activated applicator at a force of 11.0 N per array. MNs were then left within the skin for a period of 24 h and skin electrical resistance continuously monitored.

2.6. Optical coherence tomography

The depth of the pore created following the application, and removal, of PMVE/MA MNs to full thickness neonatal porcine skin at a force of 11.0 N per array was determined using optical coherence tomography (OCT) (VivoSight® high resolution OCT scanner with handheld probe (Michelson Diagnostics Ltd, Kent, UK), as described previously [19]. The swept-source Fourier domain OCT system has a laser centre wavelength of 1305.0 ± 15.0 nm, facilitating real time high resolution imaging of the upper skin layers (7.5 μm lateral and 10.0 μm vertical resolution). The skin model was scanned at a rate of up to 15 B-scans (2D cross-sectional scans) per second (scan width = 2.0 mm). 2D images were analysed using the imaging software ImageJ®. The scale of the image files obtained was 1 pixel = 4.2 μm, thus allowing accurate measurements of the depth of MN penetration, the width of the pore created, and the distance between the MN base plate and the *stratum corneum*. To allow differentiation between MN and skin model layers false colours were applied using Ability Photopaint® Version 4.14 (Ability Plus Software Ltd, Crawley, UK). In all instances, five replicates were performed and > 5 MN measured for each replicate.

2.7. Statistical analysis

Where appropriate, data were analysed using a one-way analysis of variance (ANOVA), with *post-hoc* comparisons using Tukey's HSD test. In all cases, $p<0.05$ denoted significance. Statistical Package for the Social Sciences, SPSS 18.0 Version 2.0 (SPSS Inc, Chicago, IL, USA), was used for all analyses.

3. Results

It was found that incorporation of the model solutes into the PMVE/MA matrix produced MN arrays which were perfect replicates of the laser-engineered moulds. Fig. 2 shows SEM images of the different PMVE/MA MN array designs under investigation during the first stage of this study.

Analysis of Type 2 PMVE/MA MN arrays following incorporation of model solutes (Table 2) revealed that the actual drug content was 3.26 ± 0.12, 3.28 ± 0.09 and 3.27 ± 0.12 mg for MN arrays containing theophylline, methylene blue and fluorescein sodium, respectively. This equates to approximately 93% of the theoretical loading of 3.5 mg of drug per MN device for these model drug substances. Similarly, insulin content was found to be 4.68 ± 0.06 mg (approximatey 94% of theoretical loading of 5.0 mg per array) and FTIC-BSA content found to be 2.44 ± 0.13 mg (approximately 98% of theoretical loading of 2.5 mg per array). Furthemore, the actual drug content per MN array did not differ between each of the MN array designs ($p>0.05$ in all cases). Circular dichroism analysis (using a Jasco J-185 spectropolarimeter equppied with temperature controller, Jasco International Co. Ltd, Tokyo, Japan, with CD spectra collected over the wavelength range of 200–400 nm, as described previously [3]) of MN arrays containing insulin and FTIC-BSA also revealed that incoporation into the PMVE/MA matrix did not affect the secondary structure of these biomolecules (data not shown).

Table 3 illustrates the effect of MN design upon the % cumultative permeation of theophylline, methylene blue and fluorescein sodium across dermatomed neonatal porcine skin 6 h after MN application.

In general, it was found that an increase in MN height, at a constant density of 121 MNs/cm^2, lead to an increase in the amount of all model drug substances delivered across dermatomed neonatal porcine skin 6 h after MN application ($p<0.05$ in all cases). However, preliminary studies involving application of these MN arrays to human volunteers revealed that the application of MNs of 900 μm height was perceived to be relatively more painful than MNs of a shorter length (data not shown). As such, a length of 600 μm was chosen as the ideal MN height for evaluating the effect of MN density upon the permeation of compounds across the skin from these MN devices. Similarly, it was found that an increase in MN density led to an increase in the amount of all model drug substances delivered across dermatomed neonatal porcine skin 6 h after MN application ($p<0.05$ in all cases). Overall, for all model drug substances it was found that an MN array of 600 μm height and 361 MNs/cm^2 (i.e. Type 2 MN design) led to the greatest extent of transdermal drug delivery. As such, this MN array was chosen for subsequent incorporation of macromolecules insulin and FTIC-BSA for evaluating the potential of PMVE/MA MNs for MN mediated, and MN mediated iontophoretic transdermal drug delivery of peptide/protein agents.

It was found that, following MN application, there was a dramatic reduction in the electrical resistance of the skin. In particular, immediatelty after MN insertion the skin electrical resistance dropped from 21.76 ± 2.67 kΩ to 9.59 ± 0.85 kΩ, thus indicating the creation of low resistance pathways for faciliated drug permeation. Futhermore, OCT analysis revelead

that, when applied at a force of 11.0 N per array, these MN arrays penetrated to a depth of approximately 460 μm and created pores of surface diameter approximately 215 μm within the *stratum corneum* (Fig. 3A). Interestingly, it was found that, if these MNs were removed immediately after application, as in the case of traditional 'poke and patch' MN techniques [20], then the skin constricted such that the size of the pore remaining was significantly reduced in comparison to the true depth of which the MN had penetrated ($p<0.001$). In particular, it was found that the pore created within the skin post (< 30 s) MN removal had a depth of approximately 260 μm and a surface diameter of approximately 120 μm (Fig. 3B).

Fig. 4 illustrates the permeation profiles of the model solutes across dermatomed neonatal porcine skin from drug loaded soluble PMVE/MA MN arrays, with and without combination with ITP.

As can be appreciated from Fig. 4, the combination of MN and ITP did not further enhance the extent of small molecular weight solute delivery (theophylline, methylene blue, and fluorescein sodium) from the drug loaded soluble PMVE/MA MN arrays, where between approximately 70–80% of the incorporated drug was delivered from the MN device across the skin 6 h after MN application. However, the extent of peptide/protein permeation was significantly enhanced when ITP was used in combination with the soluble PMVE/MA MN arrays. For example, it was found that the combination of anodal ITP (given that insulin will be positively charged at the pH of the PMVE/MA formulation—pH 3.5) and MNs led to the greatest enhancement in insulin permeation, in comparison to either MN ($p<0.001$) or ITP ($p<0.001$) alone. In particular, the cumulative amount of insulin permeated across neonatal porcine skin at 6 h was found to be approximately 150 μg (3.25%), 227 μg (4.85%) and 462 μg (9.87%) for ITP, MN, and MN/ITP delivery strategies, respectively. Similarly, the combination of MN and anodal ITP (FTIC-BSA will be positively charged at pH 3.5) led to a significant increase in the rate and extent of FTIC-BSA delivery from the PMVE/MA MN array. The cumulative amount of FTIC-BSA delivered across neonatal porcine skin after a 6 h period was found to be approximately 110 μg (4.53%) for MN alone and 326 μg (13.40%) for MN in combination with anodal ITP ($p<0.001$). Moreover, it is worth highlighting that, assuming even distribution of drug between the MNs and the MN base plate, on a weight per weight ratio of MNs to MN base plate, approximately 4.5% of the overall drug loading per MN array should be contained directly within the MNs alone, with the other 95.5% distributed throughout the MN base plate. As such, it appears that, for the delivery of macromolecules, only the proportion of drug that is contained within the MNs themselves permeates across the skin, with no further drug diffusing from the MN base, when the insulin/FTIC-BSA loaded MN arrays are applied to the skin alone. It is evident, therefore, from the *in vitro* permeation profiles of insulin and FTIC-BSA that the combination of ITP and MNs enables further transdermal permeation of macromolecules distributed throughout the MN base plate.

4. Discussion

Although there are a plethora of studies utilising MN arrays, of a wide variety of designs, for transdermal drug delivery, only a small proportion of these have focused upon the role of MN geometry in controlling the rate and extent of delivery achieved. Davidson et al.

provided a comprehensive theoretical analysis of the influence of various MN parameters, such as MN shape, MN diameter, thickness, spacing between needles, MN length (representing skin penetration depth and not actual length of MNs) and coating depth (i.e., the distance from the tip that is coated with a drug film) on drug diffusion from coated MNs and its skin permeation [21]. The results indicated that skin permeability was dependent on MN penetration depth and needle centre-to-centre spacing whereas other factors did not have significant effect on skin permeation. It was concluded that use of longer and more densely arranged MNs would enhance skin permeability to a greater extent [21]. Apart from theoretical assumptions, several studies provided practical experimental data regarding the effect of MN geometry on skin permeation. Oh et al. investigated permeation of calcein across full-thickness rat skin treated with solid polycarbonate MNs of varying heights (200 μm and 500 μm) and densities (45, 99 and 154 MN/cm^2). The study demonstrated that an increase in the height of MNs from 200 μm to 500 μm resulted in the 3.5-fold and 5.5-fold increase in calcein permeation, respectively, in comparison to the control (no MN treatment). In addition, it was observed that an increase in MN density from 45 to 154 MN/cm^2 led to an increase in calcein permeation [22]. Li et al. who investigated MN-mediated transdermal transport of human IgG across hairless rat skin *in vitro* reported that IgG flux was increased approximately 4-fold when MN height was increased from 200 μm to 500 μm. Moreover, a 10-fold increase in IgG flux was seen when the number of MNs increased from 27 to 54 [23]. More recently, Yan et al. comprehensively evaluated the effect of MN length and MN density upon the permeation of acyclovir across MN pre-treated human epidermal membrane. Solid silicon MN arrays with different MN lengths (ranging from 100 to 1100 μm) and MN densities (ranging from 400 to 11,900 MNs/cm^2) were used to penetrate epidermal membrane of human cadaver skin, and the skin electrical resistance and flux of acyclovir across the pre-treated skin monitored. They reported that a linear correlation between the acyclovir flux and the skin electrical resistance was observed. MN arrays with longer needles (> 600 μm) were more effective at creating pathways across the skin and enhancing drug flux. However, the authors found that there was an optimum MN design (< 2000 MNs/cm^2) above which acyclovir flux did not increase, but rather decreased. This was attributed to the assumption that given that all MN array designs were applied to the epidermal membrane at the same force (44.5 N for 10 s) the force to an individual needle would be significantly smaller for MN arrays with high needle densities. As such, this may result in a decreased penetration of high density MN arrays into the skin [24].

Whilst the studies above eloquently highlight the importance of MN design for transdermal drug delivery enhancement, to date there has been no systematic investigation of the influence of MN geometry on the performance of drug loaded, dissolving, polymeric MN arrays which are designed to remain in contact with the skin during the period of drug delivery. Furthermore, it has recently been proposed that the combination of skin barrier impairment using microneedles coupled with iontophoresis may broaden the range of drugs suitable for transdermal delivery, as well as enabling the rate of delivery to be achieved with precise electronic control [13,16]. Whilst the combination of MN and ITP technology has shown to lead to a synergistic enhancement in the transdermal delivery of a range of molecules [13,15–17,25] no reports exist on the combination of ITP with *in situ* polymeric MN delivery systems. As such, this study evaluated effect of MN geometry upon the rate of

transdermal delivery of model solutes incorporated into soluble PMVE/MA MN arrays, with the aim of selecting an optimum MN design for the combination of polymeric MNs and ITP for enhanced macromolecular delivery in a one step process.

It was found that, for small molecular weight (< 500 Da) drug molecules (theophylline, methylene blue and fluorescein sodium), all designs of the soluble PMVE/MA MN system were capable of delivering not only the drug which was contained within the MNs themselves, but also drug which had been incorporated into the MN base plate as well. For example, following the application of Type 2 drug loaded MN arrays, the cumulative % amount of the drug loaded into the whole MN device that was delivered within 6 h after MN application was found to be approximately 82%, 80% and 73% for theophylline, methylene blue and fluorescein sodium, respectively. Given that only approximately 4.5% of the overall drug loading will be contained within the MNs themselves for the Type 2 MN design, it is clear that the vast majority of the drug contained within the MN base plate was capable of traversing the MN channels and across the skin. This finding would suggest that, following MN insertion, this polymeric formulation is sufficiently hygroscopic to allow extraction of skin interstitial fluid to liberate and mobilise the diffusion of small molecular weight drugs contained in the MN base plate on the outer skin layer through the *in situ* MN channels. A similar scenario has been reported before for soluble MN systems [26]. The results of the *in vitro* drug release investigations from soluble PMVE/MA MN across dermatomed neonatal porcine skin also revealed that the extent of transdermal delivery was dependent upon the design of the MN array employed. It can be seen from Table 3 that increasing MN height (within the range 350 to 900 μm) led to an increase in the extent of transdermal drug delivery achieved 6 h after MN application. This is not surprising, given the fact that an increase in MN height has previously been shown to lead to an increase in the depth of MN penetration into skin [19]. It was also found that increasing MN density from 121 to 361 MNs per array led to an increase in transdermal drug delivery of all three solutes under investigation (Table 3). There are a number of factors that contribute to this increase in drug delivery. We have previously shown that, when applied at a force of 11.0 N per array, the laser engineered MN arrays used within this study of 600 μm height penetrate to the same depth within neonatal porcine skin, irrespective of MN density [19]. As such, given that drug molecules have been directly incorporated into the soluble PMVE/MA MNs, following MN insertion into skin an increase in MN density would be associated with a greater bolus drug deposition into the same skin layer during MN dissolution. Furthermore, the increased number of microchannels created within skin by the higher density MN arrays would facilitate the enhanced diffusion of the drug contained within the MN base plate residing on the upper skin surface [22,24,26].

Overall, the *in vitro* permeation studies revealed that the Type 2 MN design (containing 361 MNs/cm^2 of 600 μm height) resulted in the greatest extent of transdermal drug delivery. As such, this design was evaluated for its potential in the MN mediated iontophoretic transport of both small molecular weight drug molecules and peptide/protein macromolecules. It was shown that the application of these MN arrays to skin caused the skin electrical resistance to decrease from approximately 22 kΩ to approximately 9.6 kΩ. As such, the creation of these pathways of low electrical resistance should facilitate enhanced drug permeation following

the application of an electric current [13]. Whilst it was found that the combination of ITP and MN did not lead to a further enhancement in the extent of small molecular weight drug delivery achieved from the drug loaded soluble PMVE/MA MN array, it was found that the application of an electric current significantly increased the extent of macromolecular delivery from the PMVE/MA MN array. Wu et al. reported a similar finding, whereby whilst the transdermal permeation of high molecular weight compounds through MN induced channels could be increased through the combination of ITP, there was no significant increase in the permeation of low molecular weight compounds that were otherwise passively permeating to a high degree through the MN induced channels [16]. Interestingly, there was a notable difference in the permeation profile of the macromolecules, insulin and FTIC-BSA, released from the PMVE/MA MNs in comparison to the release of the small molecular weight compounds. In particular, although almost the entire drug incorporated through the MN matrix was delivered in the case of small molecular weight compounds, it was found that, for MN delivery alone, it appears that only the quantity of insulin and FTIC-BSA that was contained within the MNs themselves (and not the MN base plate) was released across the skin. A potential reason for this could be that following MN insertion, the MNs embedded with the skin rapidly dissolve releasing their macromolecular drug payload. Subsequently, the uptake of fluid by the PMVE/MA MN array may lead to the formation of a gel plug residing within the created MN channels, through which large peptide/protein agents may have a low diffusivity [3]. Importantly, however, it appears that the application of an electric current to the drug loaded PMVE/MA MNs enables efficient delivery of peptide/protein agents through these polymeric MN channels. This may be due to a combination of direct electromigratory action on the drug molecule (both insulin and FTIC-BSA are positively charged at the pH of the PMVE/MA formulation—approximately 3.5) or, potentially, the establishment of an electro-osmotic flow (in the anode to cathode direction) following current application may facilitate enhanced hydration of the MN base plate thus enhancing the mobility of the incorporated drug through the PMVE/MA MN matrix [27].

Whilst previous studies have demonstrated a synergistic enhancement in the transdermal delivery of a wide range of drug species through the combination of MN and ITP [13,15,16,25] there are a number of notable advantages of the use of drug loaded soluble MN arrays. To date, MNs have only been utilised to puncture the skin, thus creating aqueous pores of low electrical resistance, prior to the subsequent application of a drug loaded formulation for ITP delivery. The necessity for a two-stage application when using this approach may be combersome for clinicians, and patients, particularly given the importance of ensuring that the drug loaded formulation is placed correctly over the porated skin area. Furthermore, it has been shown in this study that the process of skin healing begins almost immediately upon MN removal. In particular, the surface area of each pore created in the *stratum corneum* was shown to be greater when MNs are kept in place within the skin, in comparison to when MNs are used to merely puncture the skin and then removed, which may facilitate enhanced macromolecular delivery when combined with ITP. As such, dissolving drug loaded PMVE/MA MNs offer the potential for MN mediated iontophoretic transdermal delivery of therapeutic peptide/protein agents in a one step approach. Moreover, this study has shown that, whilst PMVE/MA MN arrays are capable of delivering the

majority of small molecular weight compounds incorporated throughout its entire matrix, only the proportion of macromolecules within the MNs themselves, and not the MN base plate are delivered when MN are applied to the skin alone. Although it may be possible to alter the manufacturing process such that peptide/protein agents are loaded only into MNs, the addition of a more complex stage for MN production may slow its progression to workable mass scale production techniques. Furthermore, it would then become essential to conduct long term stability studies to ensure peptide/protein migration from the MNs to the MN base plate did not occur upon production/storage. This study has shown that the combination of ITP, a well established technique of which industrial processes for the production of iontophoretic devices are already in existence, enables the more efficient delivery of peptide/protein molecules that are incorporated throughout the entire MN base plate matrix. Interestingly, given that further peptide/protein delivery from the MN base plate only occurs in conjunction with the application of an electric current, this may offer the possibility for the combination of dissolving drug loaded PMVE/MA MN arrays with ITP for the pulsatile delivery of therapeutic peptide/proteins.

5. Conclusion

The present study highlighted, for the first time, the importance of MN geometry upon the extent of transdermal drug delivery from drug loaded dissolving polymeric MN arrays. In particular, it was found that an increase in MN height and MN density led to an increase in the amount of drug delivered from dissolving PMVE/MA MN arrays. Furthermore, incorporation of biomacromolecules into the PMVE/MA MN matrix did not adversely affect the secondary structure of model peptide insulin or model protein FTIC-BSA.

Whilst MN pre-treatment of skin has previously been shown to increase the iontophoretic mediated delivery of a range of compounds both *in vitro* and *in vivo*, this study has shown, for the first time, the potential for ITP to be combined with polymeric MN devices that remain in contact with the skin during the course of drug delivery. Furthermore, it has been shown that the application of an electric current enables the permeation of macromolecules from the entire MN array matrix, and not just that which was contained within the MNs alone, thus significantly increasing the efficiency of peptide/protein delivery. As such, future studies will focus upon the incorporation of iontophoretic components into polymeric MN devices and their potential for efficient, electrically controlled pulsatile delivery of macromolecules from drug loaded dissolving polymeric MN arrays.

Acknowledgments

This study was supported by BBSRC grant numbers BB/FOF/287 and BB/E020534/1 and Wellcome Trust grant number WT094085MA.

References

[1]. Prausnitz MR. Microneedles for transdermal drug delivery. Adv. Drug Deliv. Rev. 2004; 56:581–587. [PubMed: 15019747]

[2]. Banga A. Theme section: transdermal delivery of proteins. Pharm. Res. 2007; 24:1357–1359. [PubMed: 17492493]

[3]. Migalska K, Morrow DIJ, Garland MJ, Thakur R, Woolfson AD, Donnelly RF. Laser-engineered dissolving microneedle arrays for transdermal macromolecular drug delivery. Pharm. Res. 2011; 28:1919–1930. [PubMed: 21437789]

[4]. Kaushik S, Allen H, Donald D, McAllister D, Smitra S, Allen M, Prausnitz MR. Lack of pain associated with microfabricated microneedles. Anesth. Analg. 2001; 92:502–504. [PubMed: 11159258]

[5]. Bal SM, Caussin J, Pavel S, Bouwstra JA. *In vivo* assessment of safety microneedle arrays in human skin. Eur. J. Pharm. Sci. 2008; 35:193–202. [PubMed: 18657610]

[6]. Van Damme P, Oosterhuis-Kafeja F, Van der Wielen M, Almagor Y, Sharon O, Levin Y. Safety and efficacy of a novel microneedle device for dose sparing intradermal influenza vaccination in healthy adults. Vaccine. 2009; 27:454–459. [PubMed: 19022318]

[7]. Wilke N, Mulcahy A, Ye S, Morrissey A. Process optimization and characterization of silicon microneedles fabricated by wet etch technology. Microelectronics J. 2005; 36:650–656.

[8]. McAllister D, Wang P, Davis S, Park J, Canatella P, Allen M, Prausnitz M. Microfabricated needles for transdermal delivery of macromolecules and nanoparticles: fabrication methods and transport studies. PNAS. 2003; 100:13755–13760. [PubMed: 14623977]

[9]. Cormier M, Johnson B, Ameri M, Nyam K, Libiran L, Zhang D, Daddona P. Transdermal delivery of desmopressin using a coated microneedle array patch system. J. Control. Release. 2004; 97:503–511. [PubMed: 15212882]

[10]. Sullivan S, Murthy N, Prausnitz MR. Minimally invasive protein delivery with rapidly dissolving polymer microneedles. Adv. Mater. 2008; 20:933–938. [PubMed: 23239904]

[11]. Chu L, Choi S, Prausnitz MR. Fabrication of dissolving polymer microneedles for controlled drug encapsulation and delivery: bubble and pedestal microneedle designs. J. Pharm. Sci. 2010; 99:4228–4238. [PubMed: 20737630]

[12]. Donnelly RF, Majithiya R, Singh TRR, Morrow DIJ, Garland MJ, Demir YK, Migalska K, Ryan E, Gillen D, Scott C, Woolfson AD. Design, optimization and characterization of polymeric microneedle arrays prepared by a novel laser-based micromoulding technique. Pharm. Res. 2011; 28:41–57. [PubMed: 20490627]

[13]. Lanke S, Kolli C, Strom J, Banga A. Enhanced transdermal delivery of low molecular weight heparin by barrier perturbation. Int. J. Pharm. 2009; 365:26–33. [PubMed: 18801420]

[14]. Wang Y, Thakut R, Fan Q, Michniak B. Transdermal iontophoresis: combination strategies to improve transdermal iontophoretic drug delivery. Eur. J. Pharm. Biopharm. 2005; 60:179–191. [PubMed: 15939232]

[15]. Katikaneni S, Badkar A, Nema S, Banga AK. Molecular charge mediated transport of a 13 kD protein across microporated skin. Int. J. Pharm. 2009; 378:93–100. [PubMed: 19501142]

[16]. Wu XM, Todo H, Sugibayashi K. Enhancement of skin permeation of high molecular compounds by a combination of microneedle pretreatment and iontophoresis. J. Control. Release. 2007; 118:189–195. [PubMed: 17270306]

[17]. Chen H, Zhu H, Zheng J, Mou D, Wan J, Hang J, Shi T, Zhao T, Xu H, Yang X. Iontophoresis-driven penetration of nanovesicles through microneedle-induced skin microchannels for enhancing transdermal delivery of insulin. J. Control. Release. 2009; 139:63–72. [PubMed: 19481577]

[18]. Garland MJ, Thakur RRS, Woolfson AD, Donnelly RF. Electrically enhanced solute permeation across poly (ethylene glycol)-crosslinked poly (methyl vinyl ether-co- maleic acid) hydrogels: effect of hydrogel crosslink density and ionic conductivity. Int. J. Pharm. 2011; 406:91–98. [PubMed: 21236323]

[19]. Donnelly RF, Garland MJ, Morrow DIJ, Migalska K, Singh TRR, Majithiya R, Woolfson AD. Optical coherence tomography is a valuable tool in the study of the effects of microneedle geometry on skin penetration characteristics and in-skin dissolution. J. Control. Release. 2010; 147:333–341. [PubMed: 20727929]

[20]. Garland MJ, Migalska K, Mahmood TMT, Singh TRR, Woolfson AD, Donnelly RF. Microneedle arrays as medical devices for enhanced transdermal drug delivery. Expert Rev. Med. Devices. 2011; 8:459–482. [PubMed: 21728732]

[21]. Davidson A, Al-Qallaf B, Das DB. Transdermal drug delivery by coated micro-needles: geometry effects on effective skin thickness and drug permeability. Chem. Eng. Res. Des. 2008; 86:1196–1206.

[22]. Oh J, Park H, Do K, Han M, Hyun D, Kim C, Lee S, Hwang S, Shin S, Cho C. In-fluence of the delivery systems using a microneedle array on the permeation of a hydrophilic molecule, calcein. Eur. J. Pharm. Biopharm. 2008; 69:1040–1045. [PubMed: 18411045]

[23]. Li G, Badkar A, Nema S, Kolli CS, Banga AK. *In vitro* transdermal delivery of therapeutic antibodies using maltose microneedles Int. J. Pharm. 2009; 368:109–115.

[24]. Yan G, Warner K, Zhang J, Sharma S, Gale K. Evaluation of needle length and density of microneedle arrays in the pretreatment of skin for transdermal drug delivery. Int. J. Pharm. 2010; 391:7–12. [PubMed: 20188808]

[25]. Vemulapalli V, Yang Y, Friden PM, Banga AK. Synergistic effect of iontophoresis and soluble microneedles for transdermal delivery of methotrexate. J. Pharm. Pharmcol. 2008; 60:27–33.

[26]. Lee JW, Park JH, Prausnitz MR. Dissolving microneedles for transdermal drug delivery. Biomaterials. 2008; 29:2113–2124. [PubMed: 18261792]

[27]. Pikal M. The role of electroosmotic flow in transdermal iontophoresis. Adv. Drug Deliv. Rev. 2001; 46:281–305. [PubMed: 11259844]

Europe PMC Funders Author Manuscripts

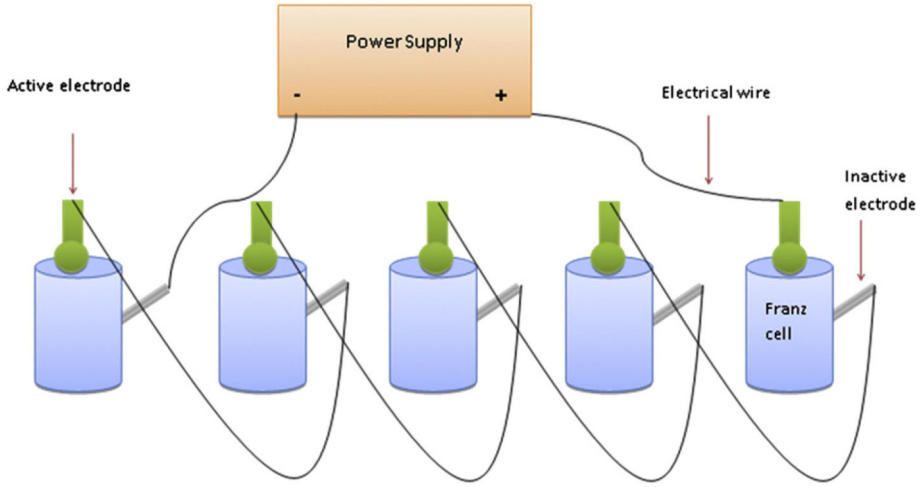

Fig. 1. Schematic illustration of experimental set up employed during iontophoretic investigations.

Europe PMC Funders Author Manuscripts

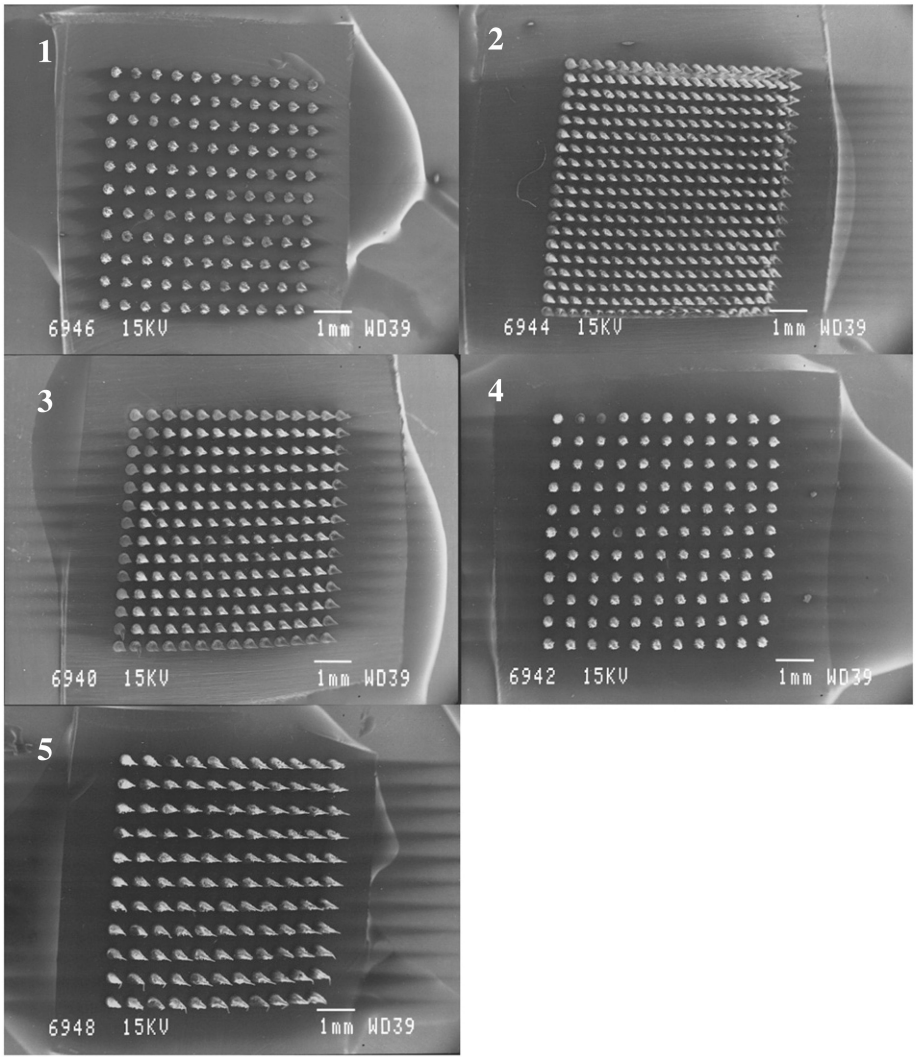

Fig. 2. SEM images of laser engineered PMVE/MA MN arrays, showing MN Type 1 (MN Height 350 μm, MN interspacing 300 μm) (1), Type 2 (MN Height 600 μm, MN interspacing 50 μm) (2), Type 3 (MN Height 600 μm, MN interspacing 150 μm) (3), Type 4 (MN Height 600 μm, MN interspacing 300 μm) (4), Type 5 (MN Height 900 μm, MN interspacing 300 μm) (5).

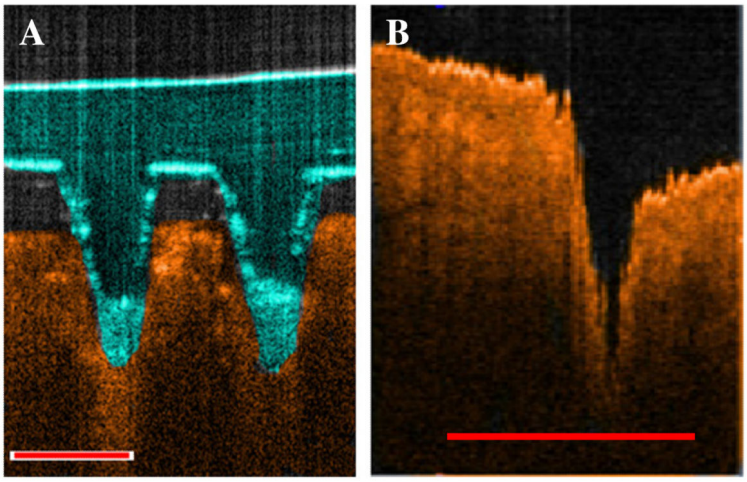

Fig. 3. Representative OCT images of PMVE/MA MN penetration into dermatomed neonatal porcine skin (A), and the pore created within the skin following MN removal (B).
Scale bar represents a length of 300 μm.

Europe PMC Funders Author Manuscripts

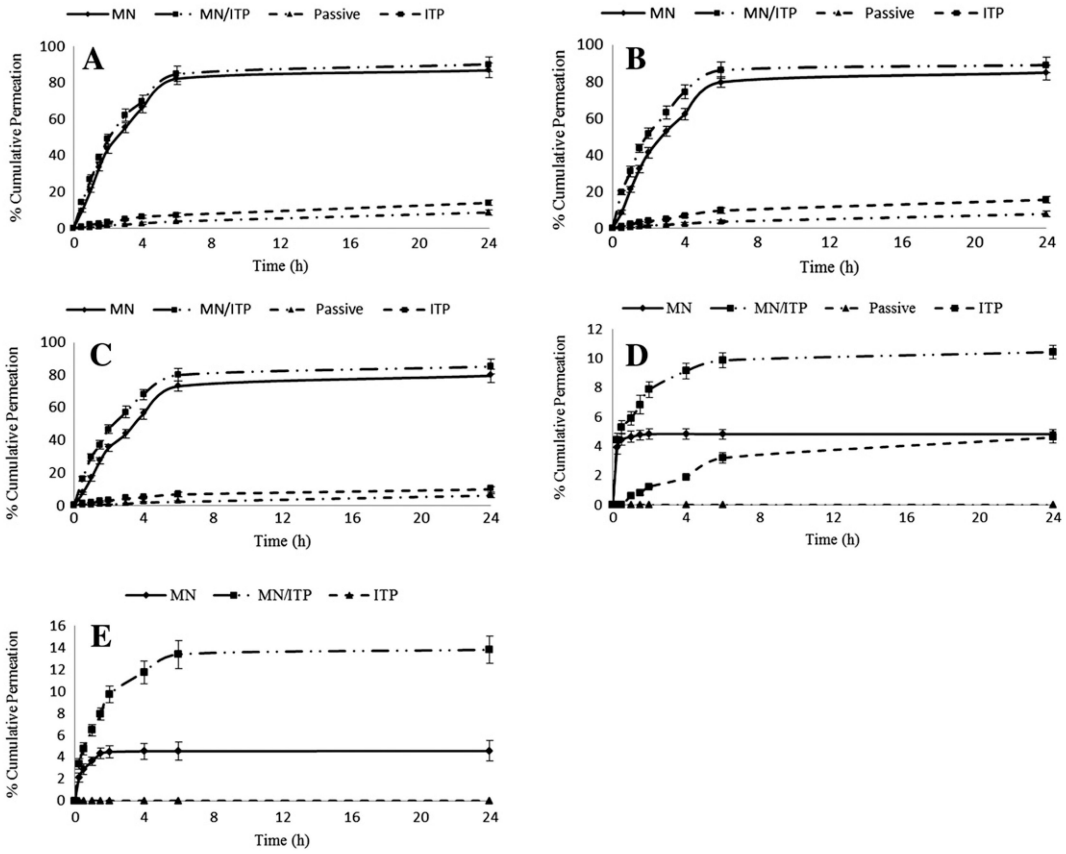

Fig. 4. ***In vitro*** **permeation profile of (A) theophylline, (B) methylene blue, (C) fluorescein sodium, (D) insulin, and (E) FTIC-BSA from drug loaded soluble PMVE/MA MN arrays (Type 2) across dermatomed neonatal porcine skin, with and without the combination of ITP.**
(Mean ± SD, *n* = 5).

Europe PMC Funders Author Manuscripts

Europe PMC Funders Author Manuscripts

Table 1

Summary of MN array designs prepared for subsequent evaluation.

MN type	MN height (μm)	MN width at base (μm)	MN interspacing at base (μm)	MN density (MNs/cm^2)*
1	350	300	300	121
2	600	300	50	361
3	600	300	150	196
4	600	300	300	121
5	900	300	300	121

*MN density of 121 MNs/cm^2 is equivalent to an 11 × 11 array, 196 MNs/cm^2 equivalent to a 14 × 14 array, and 361 MNs/cm^2 equivalent to a 19 × 19 array.

Europe PMC Funders Author Manuscripts

Table 2

Actual drug content of the model solutes loaded into Type 2 PMVE/MA MN arrays.

(Mean ± SD, n = 5).

Drug	Theoretical drug content (mg)	Actual drug content (mg)	% of theoretical drug content
Theophylline	3.50	3.26 ± 0.12	93.14 ± 3.43
Methylene blue	3.50	3.28 ± 0.09	93.71 ± 2.57
Fluorescein sodium	3.50	3.27 ± 0.12	93.43 ± 3.43
Insulin	5.00	4.68 ± 0.06	93.60 ± 1.20
FTIC-BSA	2.50	2.44 ± 0.13	97.60 ± 5.20

Europe PMC Funders Author Manuscripts

Table 3

% Cumulative amount of model solutes permeated across dermatomed neonatal porcine skin from drug loaded PMVE/MA MN arrays.

(Mean ± SD, n = 5).

Variable	Cumulative % permeated at 6 h		
	Theophylline	**Methylene blue**	**Fluorescein sodium**
MN height (μm) *			
350	52.75 ± 1.48	49.07 ± 1.82	38.39 ± 2.77
600	65.19 ± 2.63	63.38 ± 2.53	54.68 ± 4.61
900	72.48 ± 3.01	71.21 ± 1.97	62.51 ± 5.13
MN Density (MNs/cm^2) **			
121	65.19 ± 2.63	63.38 ± 2.53	54.68 ± 4.61
196	73.67 ± 2.91	69.82 ± 1.93	67.06 ± 3.85
361	82.14 ± 3.15	79.65 ± 2.77	73.19 ± 2.99
Control patch	3.52 ± 0.87	3.36 ± 0.59	2.27 ± 0.48

* Constant MN density of 121 MNs/cm^2.

** Constant MN height of 600 μm.